

LEGIBILITY NOTICE

A major purpose of the Technical Information Center is to provide the broadest dissemination possible of information contained in DOE's Research and Development Reports to business, industry, the academic community, and federal, state and local governments.

Although portions of this report are not reproducible, it is being made available in microfiche to facilitate the availability of those parts of the document which are legible.

Los Alamos National Laboratory is operated by the University of California for the United States Department of Energy under contract W-7405-ENG-36

TITLE: OSCILLATING VIRTUAL CATHODE, LARGE ORBIT GYROTRON AND DRIVER

AUTHOR(S): F. W. VanHaaften, R. F. Hoeberling, M. V. Fazio

SUBMITTED TO: The National Conference on High Power Microwave Technology for Defense Applications, Kirtland Air Force Base, Albuquerque, NM, December 1-5, 1986

DISCLAIMER

This report was prepared as an account of work sponsored by an agency of the United States Government. Neither the United States Government nor any agency thereof, nor any of their employees, makes any warranty, express or implied, or assumes any legal liability or responsibility for the accuracy, completeness, or usefulness of any information, apparatus, product, or process disclosed, or represents that its use would not infringe privately owned rights. Reference herein to any specific commercial product, process, or service by trade name, trademark, manufacturer, or otherwise does not necessarily constitute or imply its endorsement, recommendation, or favoring by the United States Government or any agency thereof. The views and opinions of authors expressed herein do not necessarily state or reflect those of the United States Government or any agency thereof.

By acceptance of this article, the publisher recognizes that the U.S. Government retains a nonexclusive, royalty-free license to publish or reproduce the published form of this contribution or to allow others to do so for U.S. Government purposes.

The Los Alamos National Laboratory requests that the publisher identify this article as work performed under the auspices of the U.S. Department of Energy.

 **Los Alamos** Los Alamos National Laboratory
Los Alamos, New Mexico 87545

MASTF

F. W. VanHaften, R. F. Hoeberling, M. V. Fazio, AT-5, MS H827
Los Alamos National Laboratory, Los Alamos, NM 87545

Introduction

Studies using an oscillating virtual cathode (vircator) and a large-orbit gyrotron to generate microwave levels of several hundred megawatts are being conducted at the Los Alamos National Laboratory (LANL). A pulse level of ~1 MV, with length approaching 1 μ s at a repetition rate of a few hertz, is anticipated for extension of these studies from the present single-shot mode with 100-ns pulse width. The increased pulse width is needed to test longer pulse length microwave sources. Pulse forming network (PFN), transformer-coupled drivers have been studied and are part of the subject of this paper. The large-orbit gyrotron is discussed here, and the vircator is the subject of Ref. 1.

Large-Orbit Gyrotron - A Summary

The conventional magnetron was the first crossed-field electron tube to generate high-power coherent microwave radiation at decimeter and centimeter wavelengths. The cross section of a typical magnetron is shown in Fig. 1a. A voltage is applied between the coaxial center cathode and the anode vanes. Electrons are emitted from the cathode and circulate, azimuthally, into the interaction space. This motion results from the $E \times B$ drift velocity caused by the presence of the axial magnetic field. Microwave radiation is produced by the resonant interaction between the circulating space charge and the magnetron modes associated with the anode slow-wave structure. These modes correspond to integral numbers of wavelengths around the structure.

Those rf waves that have phase velocities nearly equal to the electron drift velocity can interact very strongly with the electrons. These rf field-produced forces cause azimuthal electron bunching and particle drift, either toward the anode or the cathode depending on the phase of the interaction. These rotating electron "spokes" supply additional energy to the rf field, which produces further electron bunching. The essential feature of the magnetron is that the electron bunches drift in synchronism with the rf waves supported by the anode structure. In this way, the electrical potential energy associated with the radial dc electric field is converted to rf energy.

High-power magnetrons of this type have produced over 1 GW of radiated power at 5 GHz and have been designed around various operational limitations imposed by such systems. These limitations include the following:

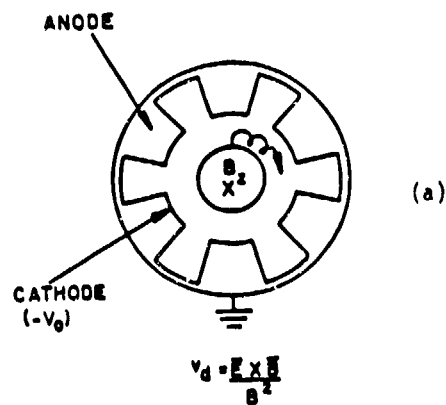
- The applied magnetic field must be large enough to prevent electrons from crossing the anode-cathode gap (the Hull criterion).
- The magnetic field must be low enough to allow space-charge circulation at a drift velocity comparable to the phase velocity of the magnetron mode to be excited (the Buneman-Hartree condition).
- The anode-cathode gap must be small enough to allow field emission of electrons from the

cathode in sufficient quantities to match the effective magnetron load impedance to the source impedance.

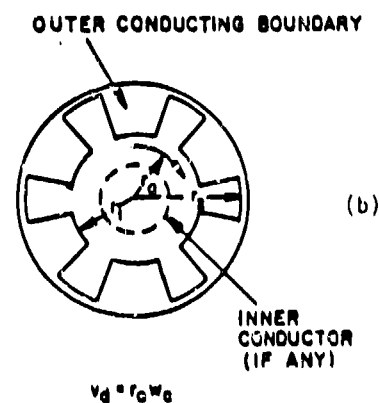
The high applied potentials in such systems must be less than a value that would induce dc and rf breakdown.

The result of these design requirements is that such devices do not perform well at higher frequencies, in part because of the slow circulation velocity of the space charge and in part because electrical breakdown and other considerations limit to a maximum of about eight the number of resonators that can be used.

In a large-orbit gyrotron (Fig. 1b), a rotating relativistic electron layer is produced by passing a hollow nonrotating beam through a narrow symmetric



CONVENTIONAL
MAGNETRON



ROTATING ELECTRON LAYER
IN A MAGNETRON-TYPE
WAVEGUIDE

Fig. 1. Comparison of conventional magnetron with large-orbit gyrotron.

*Work supported by the U.S. Department of Energy.

magnetic cusp. Radiation is again produced by resonant interaction of circulatory space charge and the magnetron modes, and the circulation is at the relativistic cyclotron frequency. Such a system has a number of advantages over conventional magnetrons:

- Much lower magnetic fields need to be applied to operate at a given microwave frequency. The space-charge drift velocity is now given by $r_0 \omega_c$, where r_0 is the mean beam radius and ω_c is the relativistic cyclotron frequency (note that the Hull criterion does not apply here and this results in field requirements of approximately 1 kG).
- The size of the device is not determined by diode impedance matching requirements and/or frequency selection considerations.
- There are no applied voltages in the interaction region and, therefore, less likelihood of dc and rf breakdown.
- The e-beam diode can be separately optimized for several microsecond operation.

As a result of all of the above, efficient higher frequency operation should be possible.

Substantial microwave powers already have been produced with this type of microwave tube. Reported results include 400 MW being produced at 10 GHz for 5 ns with 10% efficiency in a 12-slot device. Operation up to 35 GHz also has been demonstrated at the several-megawatt power level. At the lower frequencies, a three-slot device has been operated successfully at 2 GHz for 80-ns pulses. The present pulse length achieved has been limited by the electron beam machine without any evidence of diode closure. The operation of this device in a well-defined microwave mode reduces the mode conversion and waveguide transmission problems associated with some high-power microwave sources.

PFM, Transformer-Coupled Driver

A PFM transformer-coupled driver circuit is being designed to permit longer periods of operation for the microwave source, Fig. 2a. Source loading is about 50Ω for this unit. To keep the impedance of the PFM reasonable, a voltage gain of no more than 10 was deemed necessary, thus making the PFM impedance 0.5Ω . Discussions with a transformer manufacturing firm have indicated that a tightly coupled iron core unit can be fabricated with a lumped secondary leakage inductance of approximately $50 \mu\text{H}$. To accomplish this, the low side of the primary circuit cannot be isolated from the secondary circuit.

A two-section, Type C, Guillemin network shown in Fig. 2b was selected for the PFM design. This PFM design is more tolerant than others of the higher inductances needed for two-stage Marx generator arrangements required to keep dc charging voltages at a level of 100 kV. Figure 3 contains the waveform used as a design goal. It is described as having a parabolic rise and fall with a flat top. There is more rapid convergence of the pulse shape than with other waveforms, thus requiring less PFM sections. The pulse parameters T and a are defined in Fig. 3. In this paper T was taken as $1.5 \mu\text{s}$ and the parameter a as $0.1 T$. The component values of the PFM are shown in Table I. The general approach of this design is described in Ref. 2.

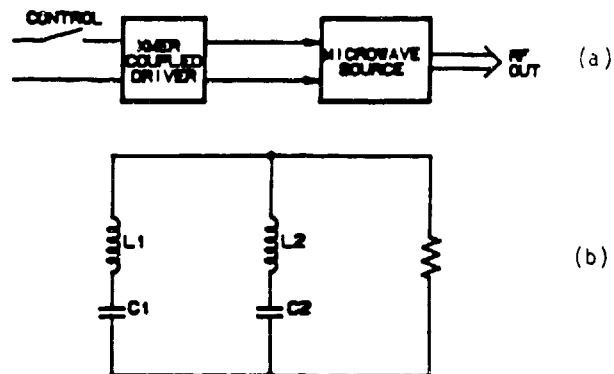


Fig. 2a. System block diagram.

Fig. 2b. Type C Guillemin network for driving transformer.

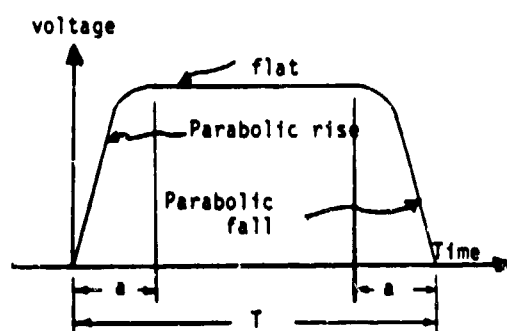


Fig. 3. Idealized driver waveform.

TABLE I

COMPONENT VALUES FOR TYPE C PFM

Component	Value
C1	1.21 μF
C2	0.125 μF
L1	189 nH
L2	202 nH

The slow rise time caused by the transformer leakage inductance will tend to distort the pulse shape considerably. The undistorted and distorted waveforms are shown in Fig. 4.

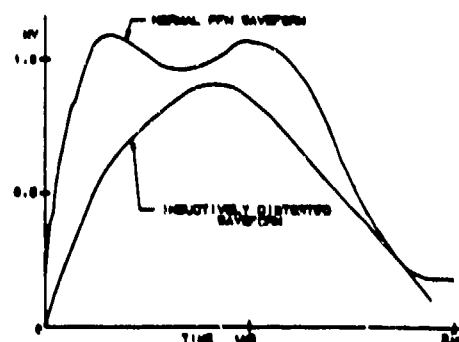


Fig. 4. PFM output waveform normal and distorted.

To further study this problem, the network was simulated using the Laboratory's NET3 Network Analysis Program. A peaking capacitor was introduced into the simulation at the output of the transformer (see Fig. 5) output and a switch was placed between the transformer output and the microwave source load resistance. The circuit is shown in Fig. 5. The optimal capacitance (CP) was found to be 10 nF with the

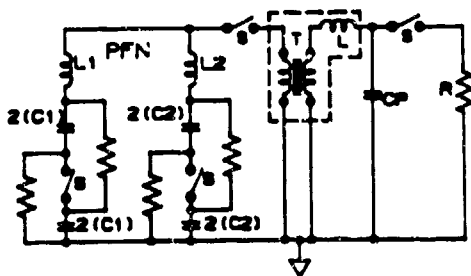


Fig. 5. Microwave source driver circuit used for modeling:

PFN: Guillemin Type C network
T: Pulse transformer
L: Transformer leakage inductance
CP: Peaking capacitance
R: Microwave source load
S: Switch

switch closing ~850 ns after closing of the PFN switches. The output voltage waveform is shown in Fig. 6. A cylindrical coaxial water capacitor 1.2 m in diameter and 2 m long can supply the capacitance needed with a sufficiently low breakdown probability.³

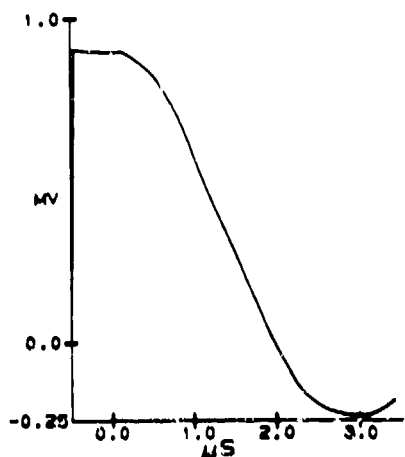


Fig. 6. Calculated single-unit output waveform.

Switching

Development will be needed in this area. For the low inductance needed in the PFN switches, either rail gap switches or parallel switches will be needed. Constant air flow for cooling and for sweeping discharge products away will be needed for all switches. The two high-current gaps in the transformer primary circuit will be a point of difficulty. For long life, the electrode material should be of the sintered tungsten-copper materials such as that developed for the Antares CO₂ Laser program.⁴ Thyatron technology is now entering the realm in which it may handle the

transformer primary switching requirements. Trigatron triggering, if any at all is needed, should be adequate for the secondary output switch. Laser triggering may be considered here.

Parallel Systems

To increase the output of the system and not increase the number of PFN Marx stages or charge voltage per stage, more than one transformer-coupled PFN assembly may be used in parallel to drive the output load. This has the added advantage of lower current gaps and higher PFN inductances. When the units are connected in parallel, the driving impedance is reduced.

Three assemblies operating in parallel were studied so that each section drives an impedance of 150 Ω, three times the desired value. The circuit for each section is identical to that of Fig. 5 except that component values are changed to account for the higher impedance. The new PFN components are found in Table II. With the three devices in parallel, matching the loading value for the microwave source (50 Ω) will be achieved.

TABLE II

COMPONENT VALUES FOR TYPE C PFN ($Z = 1.5 \Omega$)

Component	Value
C1	0.4 μ F
C2	0.040 μ F
L1	564 nH
L2	573 nH

The output waveform using no peaking capacitance and switching is shown in Fig. 7. Still some wave correction is needed. The optimum peaking capacitance

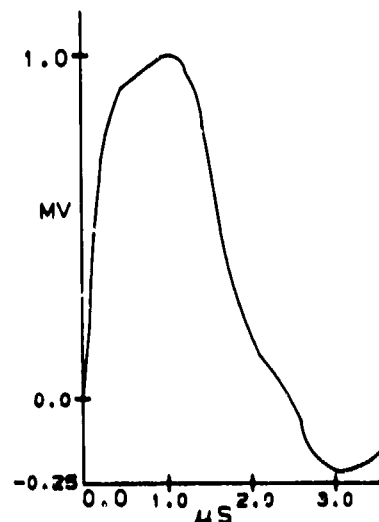


Fig. 7. Calculated output waveform for three parallel similar assemblies.

was found to be ~2 nF with the switching time at 480 ns after the closing of the PFN switches. The waveform, which looks acceptable for operation of the driver, is shown in Fig. 8. The peaking capacitor of the individual units can be combined into one, thereby making it possible to use only one output switch.

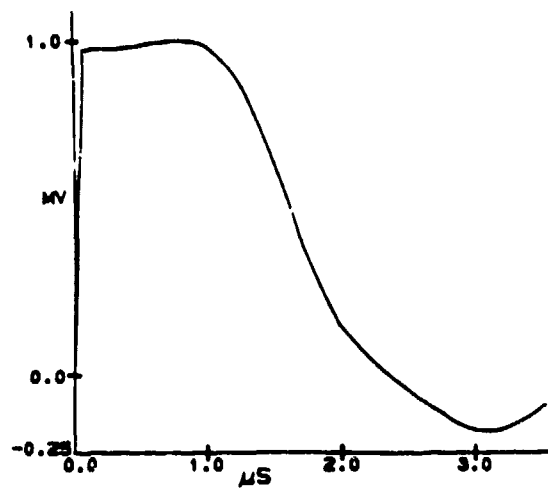


Fig. 8. Output waveform from three paralld assemblies working in unison in conjunction with peaking capacitance and output switch.

References

1. M.V. Fazio and R.F. Hoeberling, "Resonant-Cavity Operation of a Virtual-Cathode Oscillator," these proceedings.
2. MIT Radiation Laboratory Series, Pulse Generators, Chap. 6, Vol. 5, (Boston Technical Publishers, Boston, MA 1948).
3. Robert O. Hunter, Jr., Notes on Pulsed Water Systems, WRC-N-430, Western Research Corp. San Diego, CA.
4. K. B. Riepe, L. L. Barrone, K. J. Bickford, G. H. Livermore, "Antares Prototype 300-kJ, 250 kA, Marx Generator Final Report," Los Alamos National Laboratory report LA-8491 (1981).